# Effect of biquadratic coupling and in-plane anisotropy on the resonance modes of a trilayer system

A. Layadi
*Institut de Physique, Université Ferhat Abbas, Sétif 19000, Algeria*
(Received 18 July 2001; published 20 February 2002)

Ferromagnetic resonance modes are investigated for a trilayer system consisting of two ferromagnetic films interacting through a nonmagnetic interlayer. Included in the model are the bilinear $J_1$ and biquadratic $J_2$ couplings and in-plane uniaxial magnetocrystalline anisotropies with anisotropy axis directions in the two layers making a $\delta$ angle. An analytical expression for the mode intensity is derived. The saturation ($H_{sat}$) and critical ($H_{crit}$) fields, the resonant frequency, and the mode intensity are discussed as functions of $J_1$, $J_2$, and $\delta$. For a given positive $J_1$, an additional $J_2(J_2<0)$ will lead to an increase (a decrease) of the optical (acoustic) mode intensity. For fixed $J_1<0$, and if the magnetizations are parallel ($H>H_{sat}$) only the acoustic mode will appear with constant mode position and intensity for all $J_2$ values, making it difficult to detect any additional biquadratic coupling. On the other hand, and for the same parameters, if the magnetizations are antiparallel ($H<H_{crit}$), then two modes are predicted; as $|J_2|$ increases the intensity of the acoustic (optical) mode will increase (decrease), while the resonant frequency of both modes decrease.

DOI: 10.1103/PhysRevB.65.104422 PACS number(s): 76.50.+g, 76.20.+q, 75.70.Cn, 75.30.Gw

## I. INTRODUCTION

Since its observation[1] in 1986, interlayer exchange coupling has been the subject of many studies.[1,26] A typical trilayer system is composed of two ferromagnetic layers interacting through an intervening nonmagnetic interlayer. Initially, the experimental data were fitted with a bilinear coupling; in this case the magnetizations in the ferromagnetic films tend to be either parallel to each other (ferromagnetic coupling) or antiparallel (antiferromagnetic coupling). RKKY interaction could explain this kind of coupling; in this case the coupling is due to indirect exchange through conduction electrons of the intermediate layer. It is now well established that in addition to this bilinear coupling, there is a biquadratic coupling,[1–14] which can favor a perpendicular configuration of the magnetizations, i.e., a 90°-type coupling.[1–14] An angular-dependent exchange coupling, equivalent to the biquadratic coupling, was reported by Heinrich *et al.*[16] Even a third-order term was used to explain certain experimental observations.[14] The biquadratic exchange could arise from a variation of the interlayer thickness.[2,3] Magnetostatic coupling is also believed to be the source of this kind of coupling in certain systems.[4]

Several methods were used to investigate this phenomenon.[1–26] Among these techniques, ferromagnetic resonance (FMR) was widely used by several groups to study different phenomena in magnetic thin films and multilayers,[13–25,27–31] including magnetic coupling.[13–25] In earlier studies, the biquadratic coupling $J_2$ was neglected.[15–26] However, it was reported more recently that $J_2$ can be comparable to, or even larger than, the bilinear coupling[1,13] $J_1$. Also, in many papers, the in-plane anisotropy was not taken into account; in others, the easy axes of such an anisotropy were taken to be parallel. Elmers *et al.*,[8] using the magneto-optical Kerr effect, considered layers with orthogonal anisotropies.

In the present work, biquadratic coupling (in addition to the usual bilinear coupling) and in-plane uniaxial anisotropy are included; the anisotropy axes in the layers are assumed to make an arbitrary angle $\delta$ between them; situations where the anisotropies are parallel or orthogonal are illustrated as particular examples. A description of the FMR modes in such coupled layers is given. In Sec. II, general relations pertaining to FMR modes are worked out. Saturation and critical fields are introduced in Sec. III. In Sec. IV, a formula for the mode intensity is derived for this coupled system. Finally, in Sec. V, the resonance frequency and the FMR intensity are discussed as a function of the applied field $H$ and of the coupling strengths $J_1$ and $J_2$.

## II. GENERAL RELATIONS FOR FMR MODES

The two thin-film layers, denoted as $A$ and $B$, are coupled to each other through a nonmagnetic layer. The total free energy of the trilayer system per unit area can be written as[1,2,15–19]

$$E = t_A E_A + t_B E_B - J_1 \frac{\mathbf{M}_A \cdot \mathbf{M}_B}{M_A M_B} - J_2 \left( \frac{\mathbf{M}_A \cdot \mathbf{M}_B}{M_A M_B} \right)^2 . \quad (1)$$

The interlayer coupling energy is given by the two last terms. $\mathbf{M}_A$ and $\mathbf{M}_B$ denote the magnetizations of layers $A$ and $B$; $J_1$ and $J_2$ are, respectively, the bilinear and biquadratic coupling parameters. The nature and the strength of the coupling are described by the sign and the magnitude of $J_1$ and $J_2$. When $J_1$ dominates, and if it is positive, the energy is minimal when $\mathbf{M}_A$ and $\mathbf{M}_B$ are parallel (ferromagnetic coupling), while if it is negative then the lowest energy is achieved when $\mathbf{M}_A$ and $\mathbf{M}_B$ are antiparallel (antiferromagnetic coupling). If, on the other hand $J_2$ dominates and is negative (which was observed experimentally), then the minimum energy occurs when the magnetizations are oriented perpendicularly to each other (90°-type coupling[1]). Also note that this coupling analysis is a phenomenological one, with no assumption made about the origin of the coupling, even though the RKKY interaction, mainly in transition metals, can be written as a scalar product of the magnetizations[1] [as stated in the third term of Eq. (1)]. In the two first terms of

 ©2002 The American Physical Society

Eq. (1), $t_A$ and $t_B$ are the thicknesses of layers $A$ and $B$, respectively; $E_A$ and $E_B$ are the energies per unit volume of the individual layers $A$ and $B$. It is assumed that the films lie in the $x$-$y$ plane, with the $z$ axis normal to the film plane. The external applied magnetic field **H** is taken to be in the plane of the films, making an $\alpha$ angle with the $x$ axis. The microwave field **h** is along the $y$ axis. The magnetization $\mathbf{M}_A$ is defined, in spherical coordinates, by the angles $\theta_A$ and $\phi_A$; similarly $\mathbf{M}_B$ is defined by the angles $\theta_B$ and $\phi_B$. The energies $E_A$ and $E_B$ include the Zeemann energy (interaction of the external magnetic field **H** with the magnetizations) for layer $A$, $-M_A H \sin\theta_A \cos(\alpha-\phi_A)$, and the shape and any out-of-plane uniaxial anisotropy given by $K_{u\,\mathrm{eff}\,A}\sin^2\theta_A$, where $K_{u\,\mathrm{eff}\,A}=K_{uA}-2\pi M_A{}^2$, and $K_{uA}$ is the out-of-plane magnetocrystalline anisotropy constant for layer $A$. For layer $B$, in the energy $E_B$ the above relations hold by changing the subscript $A$ to $B$. Moreover the layers are assumed to have in-plane uniaxial magnetocrystalline anisotropies. For layer $A$, the easy axis of such an anisotropy is taken to be along the $x$ axis. the corresponding energy will then be $-K_A \sin^2\theta_A \cos^2\phi_A$. For layer $B$, the easy axis has an arbitrary direction within the plan, it makes a $\delta$ angle with the $x$ axis. Following the analysis in Ref. 15, the magnetocrystalline energy can be written as $-K_B \sin^2\theta_B \cos^2(\phi_B-\delta)$. $K_A$ ($K_B$) is the in-plane magnetocrystalline anisotropy constant for layer $A$ (layer $B$); $K_A$ and $K_B$ are positive, since it is assumed that the anisotropy axes are easy directions. Also, it can easily be seen that $\mathbf{M}_A$ and $\mathbf{M}_B$ must lie in the film plane due to the strong demagnetizing field of the thin films and to the fact that the applied magnetic field is in plane; thus $\theta_A=\theta_B=\pi/2$. With all these considerations, the total free energy of the system per unit area [Eq. (1)] can be explicitly written as

$$\begin{aligned}E=&t_A\{-M_A H\cos(\alpha-\varphi_A)+K_{u\,\mathrm{eff}\,A}-K_A\cos^2\varphi_A\}\\&+t_B\{-M_B H\cos(\alpha-\varphi_B)+K_{u\,\mathrm{eff}\,B}-K_B\cos^2(\varphi_B-\delta)\}\\&-J_1\cos(\varphi_A-\varphi_B)-J_2\cos^2(\varphi_A-\varphi_B).\end{aligned}\tag{2}$$

The angles $\phi_{A,B}$ are given by the following two coupled equations (the equilibrium conditions)

$$\begin{aligned}&t_A M_A H\sin(\alpha-\varphi_A)\\&\quad=t_A K_A\sin 2\varphi_A+J_1\sin(\varphi_A-\varphi_B)+J_2\sin 2(\varphi_A-\varphi_B)\end{aligned}\tag{3a}$$

and

$$\begin{aligned}&t_B M_B H\sin(\alpha-\varphi_B)\\&\quad=t_B K_B\sin 2(\varphi_B-\delta)-J_1\sin(\varphi_A-\varphi_B)-J_2\sin 2\\&\qquad\times(\varphi_A-\varphi_B).\end{aligned}\tag{3b}$$

In order to find the normal modes of the system, one can use a method based on the energy and described by Smith and Beljers.[31] In this case the equations coupling $\Delta\theta_i, \Delta\phi_i$ ($i=A$ and $B$), the excursions during oscillations about the equilibrium position, can be written in a matrix form.[15,17] The matrix elements consists of the second derivatives of the energy $E$ with respect to $\theta_i$ and $\phi_i$ ($i=A$, and $B$). A solution of the form $\exp(i\omega t)$ will be taken, $\omega$ is the (angular) frequency of precession. The solutions (normal modes) of the system will be found by setting the determinant of the matrix to zero. This will lead to a fourth-order equation in $H_R$ (the magnetic resonant field) if one is doing an experiment using a fixed frequency resonant cavity with a variable dc field. If, on the other hand, one is using a variable frequency setup (frequency sweeper) and a fixed dc field, then one may solve for the frequency. One will then find a fourth-order equation in $\omega$ (the resonant frequency) with at most two meaningful solutions (real and positive numbers) for given coupling strength parameters and dc field intensity and direction values. This latter case is worked out in the present paper. Thus, computing the second derivatives of the energy (evaluated at the equilibrium positions), setting the determinant to zero, and rearranging the terms, one will obtain a fourth-order equation in $\omega$,

$$\begin{aligned}&\left[\frac{ab}{\gamma_A\gamma_B}\right]^2\omega^4-\left[a^2b^2\left(\frac{H_1^AH_2^A}{\gamma_B^2}+\frac{H_1^BH_2^B}{\gamma_A^2}\right)\right.\\&\quad+abc_1\left(\frac{aH_2^B}{\gamma_A^2}+\frac{bH_2^A}{\gamma_B^2}\right)+abc_2\left(\frac{aH_1^B}{\gamma_A^2}+\frac{bH_1^A}{\gamma_B^2}\right)\\&\quad\left.+c_1c_2\left(\frac{a^2}{\gamma_A^2}+\frac{b^2}{\gamma_B^2}\right)+\frac{2c_0c_2ab}{\gamma_A\gamma_B}\right]\omega^2\\&\quad+[abH_2^AH_2^B+c_2(aH_2^A+bH_2^B)]\\&\quad\times[abH_1^AH_1^B+c_1(aH_1^A+bH_1^B)+(c_1^2-c_0^2)]=0\end{aligned}\tag{4}$$

where $a=t_AM_A$ and $b=t_AM_A$; $\gamma_A$ and $\gamma_B$ denote the gyromagnetic ratios of layers $A$ and $B$, respectively. The parameters $c_j$ contain the coupling strengths $c_0=J_1+2J_2\cos(\phi_A-\phi_B)$, $c_1=J_1\cos(\phi_A-\phi_B)+2J_2\cos^2(\phi_A-\phi_B)$, $c_2=J_1\cos(\phi_A-\phi_B)+2J_2\cos 2(\phi_A-\phi_B)$, and

$$H_1^A=H\cos(\alpha-\varphi_A)-H_{K\,\mathrm{eff}\,A}+H_{KA}\cos^2\varphi_A,\tag{5a}$$

$$H_2^A=H\cos(\alpha-\varphi_A)+H_{KA}\cos 2\varphi_A,\tag{5b}$$

$$H_1^B=H\cos(\alpha-\varphi_B)-H_{K\,\mathrm{eff}\,B}+H_{KB}\cos^2(\varphi_B-\delta),\tag{5c}$$

$$H_2^B=H\cos(\alpha-\varphi_B)+H_{KB}\cos 2(\varphi_B-\delta),\tag{5d}$$

where $H_{K\,\mathrm{eff}\,A}=2K_{u\,\mathrm{eff}\,A}/M_A$ ($H_{K\,\mathrm{eff}\,B}=2K_{u\,\mathrm{eff}\,B}/M_B$) and $H_{KA}=2K_A/M_A$ ($H_{KB}=2K_B/M_B$) are the effective uniaxial and the planar anisotropy fields for layer $A$ (layer $B$), respectively.

When the layers are not coupled ($J_1=J_2=0$) then $c_j=0$ and Eq. (4) will reduce to $(\omega^2-\gamma^2{}_AH^A{}_1H^A{}_2)(\omega^2-\gamma^2{}_BH^B{}_1H^B{}_2)=0$, which, upon substituting the $H^i{}_j$ by their expressions [Eqs. (5a)–(5d)] will lead to the following two uncoupled equations:

$$\left[\frac{\omega}{\gamma_A}\right]^2=[H\cos(\alpha-\varphi_A)-H_{K\,\mathrm{eff}\,A}+H_{KA}\cos^2\varphi_A]\times[H\cos(\alpha-\varphi_A)+H_{KA}\cos 2\varphi_A] \quad (6a)$$

and

$$\left[\frac{\omega}{\gamma_B}\right]^2=[H\cos(\alpha-\varphi_B)-H_{K\,\mathrm{eff}\,B}+H_{KB}\cos^2(\varphi_B-\delta)]\times[H\cos(\alpha-\varphi_B)+H_{KB}\cos 2(\varphi_B-\delta)]. \quad (6b)$$

Thus, in this uncoupled case, two peaks are expected to be observed in the FMR spectra whose positions are given by the resonance conditions [Eqs. (6a) and (6b)].

### III. SATURATION AND CRITICAL FIELDS

In this section and in the following ones, it will be assumed that the applied magnetic field is along the *x* axis, i.e., $\alpha=0$. As the field is increased, the magnetizations $\mathbf{M}_A$ and $\mathbf{M}_B$ will rotate to be parallel to $\mathbf{H}$ ($\phi_A=\phi_B=0$). Note, however, that for an arbitrary $\delta$ the magnetizations will asymptotically align with the applied field (asymptotic saturation). Only for $\delta=0$ (the easy axes in the two layers are parallel) or $\delta=90°$ (perpendicular easy axes) will the magnetizations be along $\mathbf{H}$ for a finite value of the applied field (in this case $\phi_A=\phi_B=0$ are exact solutions of the equilibrium conditions, Eqs. (3a) and (3b)). This field, the saturation field $H_{\mathrm{sat}}$, depends on the coupling strengths $J_1$ and $J_2$, on the in-plane anisotropy field intensities and directions, as well as on the thicknesses and magnetizations of both layers. From the minimization of the energy, $H_{\mathrm{sat}}$ can be found. For the simple case where the easy axes are aligned, i.e., $\delta=0$ and the anisotropy fields are equal, i.e., $H_{KA}=H_{KB}=H_K$, $H_{\mathrm{sat}}$ is found to be

$$H_{\mathrm{sat}}=-(J_1+2J_2)\left[\frac{1}{t_AM_A}+\frac{1}{t_BM_B}\right]-H_K. \quad (7)$$

When there is no biquadratic coupling ($J_2=0$) and the in-plane anisotropy is neglected ($H_K=0$), Eq. (7) reduces to relations found by Heinrich *et al.*[16] (with $M_A=M_B$) and Zhang *et al.*[17] For arbitrary values of $H_{KA}$ and $H_{KB}$ (with different $H_{KA}$ and $H_{KB}$), the saturation field is given by a more complicated formula which will not be displayed here. It can be seen from Eq. (7) that the effect of the biquadratic coupling $J_2$ (when it is negative, which is what is usually observed experimentally) is to increase the saturation field. For the parameters used in the analysis discussed in Sec. V, and for $J_1=-2$ erg/cm$^2$ and $\delta=0°$, $H_{\mathrm{sat}}$ will be equal to 4.9 and 7.7 kOe for $J_2=0$ and $J_2=-0.5$ erg/cm$^2$, respectively. Also, it can be seen from the general formula for $H_{\mathrm{sat}}$ that $H_{\mathrm{sat}}$ increases with increasing $\delta$ (with the same parameters as above, $H_{\mathrm{sat}}$ increases from 4.9 kOe for $\delta=0°$ to 5.7 kOe for $\delta=90°$ when $J_2=0$, and from 7.7 to 8.5 kOe when $J_2=-0.5$ erg/cm$^2$).

The saturation field [Eq. (7)] is valid for ferromagnetic coupling ($J_1>0$) or antiferromagnetic coupling ($J_1<0$) superposed to the biquadratic coupling $J_2$. When $J_1>0$, then $\phi_A=\phi_B=0°$ for $H>H_{\mathrm{sat}}$, while for $H<H_{\mathrm{sat}}$ the magnetization angles are given by Eqs. (3a) and (3b). When the coupling is antiferromagnetic, one still has $\phi_A=\phi_B=0°$ for $H>H_{\mathrm{sat}}$. Moreover, for this situation, one will need to define a critical field $H_{\mathrm{crit}}$ below which the magnetizations will be antiparallel under the effect of the negative coupling $J_1$. From the minimization of the energy, $H_{\mathrm{crit}}$ can be found. Once again the general formula for $H_{\mathrm{crit}}$ is quite complicated; however, it will reduce to a simpler form when $H_{KA}=H_{KB}=H_K$ and $\delta=90°$ (orthogonal anisotropy axes). In this case, $H_{\mathrm{crit}}$ is given by

$$H_{\mathrm{crit}}=-(J_1-2J_2)\left[\frac{1}{t_BM_B}-\frac{1}{t_AM_A}\right]-H_K. \quad (8)$$

It is assumed here that $t_AM_A>t_BM_B$. It can be seen that the effect of the 90°-type coupling ($J_2<0$) is to lower the critical field. For the parameters used in Sec. V, and for $J_1=-2$ erg/cm$^2$ and $\delta=0°$ and using the general formula, $H_{\mathrm{crit}}$ is found to be 3.737 and 3.691 kOe for $J_2=0$ and $-0.5$ erg/cm$^2$, respectively. Also, for given $J_1$ and $J_2$ values $H_{\mathrm{crit}}$ is found to decrease with increasing $\delta$ value (using the above parameters, $H_{\mathrm{crit}}$ will decrease from 3.737 kOe for $\delta=0°$ to 2.432 kOe for $\delta=90°$ when $J_2=0$, and from 3.691 to 0.967 kOe when $J_2=-0.5$ erg/cm$^2$), the minimal value of $H_{\mathrm{crit}}$ corresponds to $\delta=90°$ and is given by Eq. (8). Thus, for this (antiferromagnetic) coupling case, three field regions have to be defined. If $H<H_{\mathrm{crit}}$, the magnetizations are antiparallel ($\phi_A=0°$ and $\phi_B=180°$), for $H_{\mathrm{crit}}<H<H_{\mathrm{sat}}$, the magnetizations make $\phi_A$ and $\phi_B$ angles with the applied field [$\phi_A$ and $\phi_B$ are given by Eqs. (3a) and (3b)] and for $H>H_{\mathrm{sat}}$ the magnetizations are aligned along the applied field $H$ ($\phi_A=\phi_B=0°$). This fact is well described by Heinrich and co-workers[2,10–12,14] and Wigen and co-workers (e.g., Ref. 17) in specific situations (where biquadratic and in-plane anisotropy are neglected). In the present work, $H_{\mathrm{sat}}$ and $H_{\mathrm{crit}}$ are discussed for a system with biquadratic coupling and in-plane uniaxial anisotropy with arbitrary axis directions.

### IV. FMR INTENSITY

The FMR mode intensity[15,17–19,27–28] is defined as corresponding to the area under the absorption line. The intensity so defined is independent of the damping parameter value. As expected, the intensity of the coupled modes depends on the coupling strengths (bilinear and biquadratic) and on the in-plane anisotropy fields.

In the present study, the applied magnetic field $\mathbf{H}$ is parallel to the film plane, along the *x* direction, and the microwave $\mathbf{h}$ field is along the *y* direction. In this case, the magnetizations precesses in an elliptical orbit; the precession orbit is the y-z plane. The intensity is thus given by a general formula[17,19]

$$I=\frac{[\int_0^d m_y dz]^2}{\int_0^d[(m_y^2+m_z^2)/2M]dz}. \quad (9)$$

Here *m* denotes the time-dependent magnetization compo-

nent for $A$ and $B$. The coordinate along the thickness of the specimen is denoted by $z$, $d=t_A+t_B$. The FMR intensity at fixed excitation field amplitude is expected to be proportional to *magnetization times volume*, but the areas of both layers $A$ and $B$ are the same. Moreover, experimentally in any one sample we will be evaluating relative mode intensities for which the areas will cancel. Consequently the dimensions of the integral $I$ are (*magnetization times thickness*). The magnetization components $m$ are assumed to be uniform throughout each individual layer, the intensity of Eq. (9) will then be

$$I=\frac{[t_A m_{Ay}+t_B m_{By}]^2}{t_A(m_{Ay}^2+m_{Az}^2)/2M_A+t_B(m_{By}^2+m_{Bz}^2)/2M_B}. \quad (10)$$

One can compute all the four rf magnetization components by the use of the $4\times4$ matrix (see Sec. II). From the determinant of this matrix one can derive $\Delta\theta_A$, $\Delta\phi_A$, $\Delta\theta_B$, and $\Delta\phi_B$, and noting that $m_{Ay}=M_A\Delta\phi_A$, $m_{By}=M_B\Delta\phi_B$, $m_{Az}=M_A\Delta\theta_A$, and $m_{Bz}=M_B\Delta\theta_B$. After some algebraic manipulations, the rf magnetizations are computed and substituted into the intensity $I$ [Eq. (10)]. The intensity can then be put into the form

$$I=\frac{2ab\omega^2(aq+b)^2}{ab\omega^2(aq^2+b)+b\gamma_A^2[qaH_2^A+c_2(q-1)]^2+a\gamma_B^2[bH_2^B-c_2(q-1)]^2}, \quad (11a)$$

where

$$q=\frac{\gamma_A^2c_2b(aH_1^A+c_1)+\gamma_A\gamma_Bc_0a(bH_2^B+c_2)}{\gamma_A^2b(aH_1^A+c_1)(aH_2^A+c_2)+\gamma_A\gamma_Bc_0c_2a-a^2b\omega^2}. \quad (11b)$$

When the layers are uncoupled, then $c_j=0$; in this case both the numerator and denominator in $q$ are equal to zero (the denominator is equal to zero because of the resonance condition). To avoid this indetermination the intensity of each layer must be found separately. The relation for the intensity of layer $A$ is found to be

$$I_A=\frac{2M_At_A}{1+\dfrac{\omega^2}{[\gamma_AH_1^A]^2}}, \quad (12)$$

where $H^A{}_1$ is given by Eq. (5a), and $\omega$ is the angular resonant frequency. Using Eq. (5a) for layer $A$ (and assuming saturation is achieved, i.e., $\phi_A=0$) and the resonance condition [Eq. (6a)], Equation (12) can be put in a more familiar form:[15,28]

$$I_A=\frac{2M_At_A(H+H_{KA}-H_{K\,\mathrm{eff}\,A})}{(2H+2H_{KA}-H_{K\,\mathrm{eff}\,A})}. \quad (13)$$

Note that in the presence of in-plane anisotropy, the anisotropy field $H_{KA}$ appears explicitly in the intensity formula [compare Eq. (12) with those of Refs. 15 and 28]. Similar relations can be found for layer $B$.

## V. DISCUSSIONS

Equation (4) has been solved for $H$ along the $x$ axis ($\alpha=0°$). In Fig. 1, the resonant frequency is plotted against the bilinear coupling strength $J_1$ for $H>H_{\mathrm{sat}}$. In all following computations the values of $J_1$ are taken to be between 0 and 2 erg/cm$^2$, while $J_2$ is $-0.5$ erg/cm$^2$; these are about the values reported by Grünberg.[1] For the other parameters used in the computation, see the caption of Fig. 1. The solid (dashed) line corresponds to $J_2=0$ ($J_2=-0.5$ erg/cm$^2$). The curves are drawn for perpendicular in-plane anisotropy axes in the two layers ($\delta=90°$). Two modes will appear. For this ferromagnetic coupling case ($J_1>0$), the high-frequency mode (labeled in the subsequent analysis by the subscript 1) is the optical mode; its frequency will increase as $J_1$ increases. The low-frequency mode (subscript 2) is the acoustic mode; its resonant frequency will increase slightly, then level off to a limiting value as $J_1$ becomes large. Note that this is opposite to a fixed frequency analysis, where the lower resonant field corresponds to the optical mode for ferromagnetic coupling.[22] The effect of the additional biquadratic coupling $J_2$ is the decrease of the resonant frequency of both modes; as the bilinear coupling becomes strong, the resonant frequency of the acoustic mode for the two cases (with and without biquadratic coupling) will be equal (com-

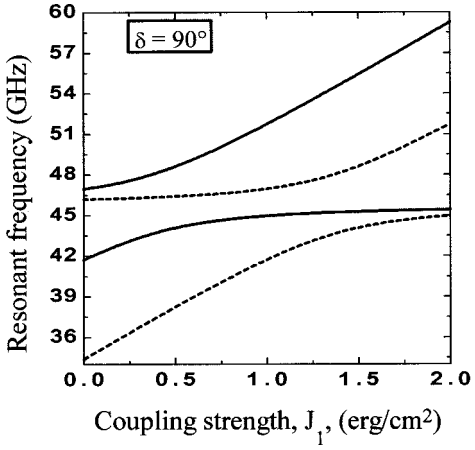


FIG. 1. Resonant frequency vs bilinear coupling strength $J_1$. $\delta=90°$ (orthogonal anisotropy axes). Solid line: $J_2=0$. Dashed line: $J_2=-0.5$ erg/cm$^2$. Layer $A$: $4\pi M_A=10$ kG, $H_{k\,\mathrm{eff}\,A}=-10$ kOe, $H_{\mathrm{KA}}=0.5$ kOe, and $\gamma/2\pi=2.8$ GHz/kOe. Layer B: $4\pi M_B=6$ kG, $H_{k\,\mathrm{eff}\,B}=-6$ kOe, $H_{\mathrm{KB}}=0.5$ kOe, and $\gamma/2\pi=2.9$ GHz/kOe. Applied field $H=12$ kOe.

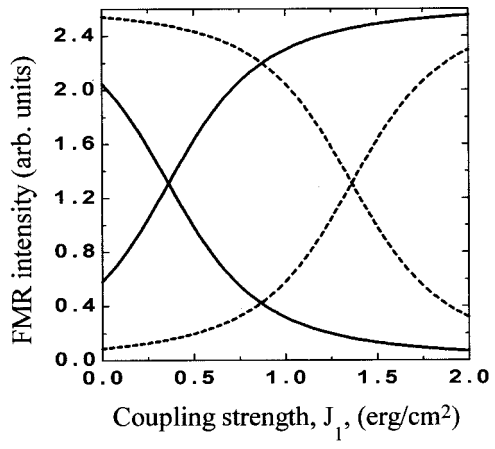


FIG. 2. FMR intensity vs bilinear coupling strength $J_1$. $\delta = 90°$ (orthogonal anisotropy axes). Solid line: $J_2 = 0$. Dashed line: $J_2 = -0.5$ erg/cm$^2$. Other parameters as in Fig. 1.

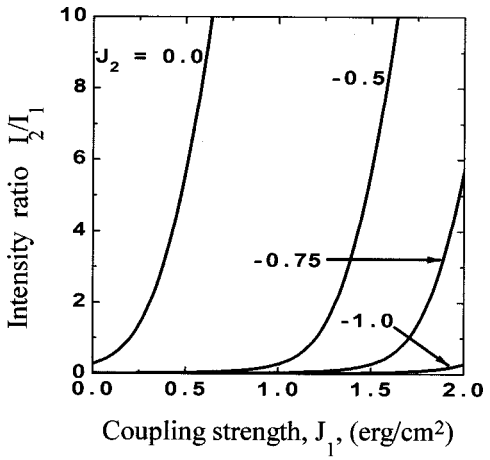


FIG. 4. Intensity ratio ($I_2/I_1$) vs bilinear coupling strength $J_1$ for different $J_2$ values (shown on the curves), $\delta = 0°$ (parallel anisotropy axes). Other parameters as in Fig. 1.

pare the solid and dashed lines in Fig. 1); i.e., in the strong $J_1$ region, $J_2$ becomes negligible compared to $J_1$. This behavior (the decrease) of the resonant frequency is the same for all $\delta$ values, (only $\delta = 90°$ case is shown in Fig. 1, as an example); however, the particular way the resonant frequency varies with $J_1$ does depend on the $J_2$ and $\delta$ values.

The corresponding mode intensities [Eqs. (11a) and 11(b)] are shown in Fig. 2. For a given $J_2$ value, as $J_1$ increases, the optical (acoustic) mode intensity will decrease (increase); at some point the mode intensities will be comparable; then, as $J_1$ becomes very strong, the optical mode intensity will go to zero while that of the acoustic mode will level off to a constant value. This variation is seen for all $J_2$ and $\delta$ values; however, the point of the reversal in intensity does depend on $J_2$ and $\delta$ as will be discussed below. Also the effect of $J_2$ on the intensity vs $J_1$ curve can be seen by comparing the solid and dashed lines in Fig. 2; as $|J_2|$ increases the optical (acoustic) mode intensity will increase (decrease).

Sometimes the difference in mode position is used to derive the coupling strength.[25] In Fig. 3, the difference in the resonance frequency, $\Delta f_R = f_1 - f_2$, is plotted against $J_1$ for several values of $J_2$ (the $J_2$ values are shown on the curves) for $\delta = 0°$. The $\Delta f_R$ vs $J_1$ curves present minima whose positions depend on the values of $J_2$; however, the minimum value of $\Delta f_R$ is independent of $J_2$. A linear variation of $\Delta f_R$ vs $J_1$ can also be observed for certain $J_1$ values. Note, however, that the difference in mode position is meaningful only if both peaks appear, i.e., if the intensities are not zero; thus one may check the intensity values first (Fig. 4). Also, for a given $\Delta f_R$ (an experimental measurement of the separation between the two peaks in an FMR spectrum), several values of $J_1$ and $J_2$ can be obtained. Even if the biquadratic coupling is fixed or is not taken into account (see the $J_2 = 0$ curve in Fig. 3) a measured $\Delta f_R$ will lead to two $J_1$ values because of the bowing of the curves. Thus deriving the coupling strength from the difference in mode position only[25] can be misleading. The mode intensity values should sometimes lift this degeneracy. Experimentally the intensity ratio is more meaningful than the absolute intensity of each mode, and is usually used in the interpretation of the data. In Fig. 4, the intensity ratio, $I_2/I_1$ vs $J_1$ is shown for different values of $J_2$ (and $\delta = 0°$). The effect of the biquadratic coupling on the mode intensity ratio is clear from this figure. Note that, as $J_1$ increases, the intensity ratio increases from almost zero (where the optical mode intensity is stronger) to a large value (where only acoustic mode will be detected), a reversal of the mode intensities will occur. The value of $J_1$ where the mode intensities are equal ($I_2/I_1 = 1$) (the reversal point) depends on the value of $J_2$, and actually corresponds to the same value where the minimum occurs in the $\Delta f_R$ vs $J_1$ curves (see Fig. 3).

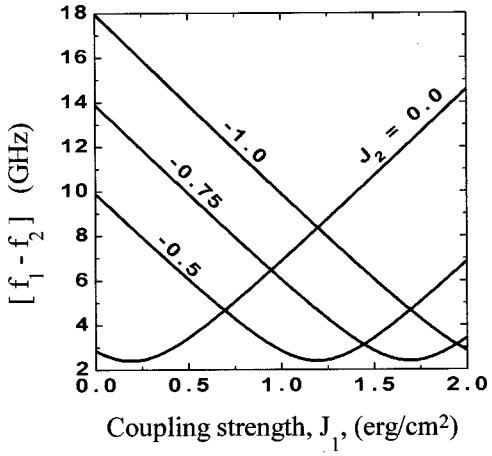


FIG. 3. Difference in mode position ($f_1 - f_2$) vs bilinear coupling strength $J_1$ for different $J_2$ values (shown on the curves). $\delta = 0°$ (parallel anisotropy axes). Other parameters as in Fig. 1.

Assume now that the coupling is antiferromagnetic ($J_1 < 0$). For a fixed coupling ($J_1 = -2$ erg/cm$^2$), the problem is to see the effect of an additional biquadratic coupling ($J_2$ from 0 to $-0.5$ erg/cm$^2$) on the FMR mode position and intensity. In this (antiferromagnetic) coupling situation, the higher (lower) frequency mode is the acoustic (optical) mode

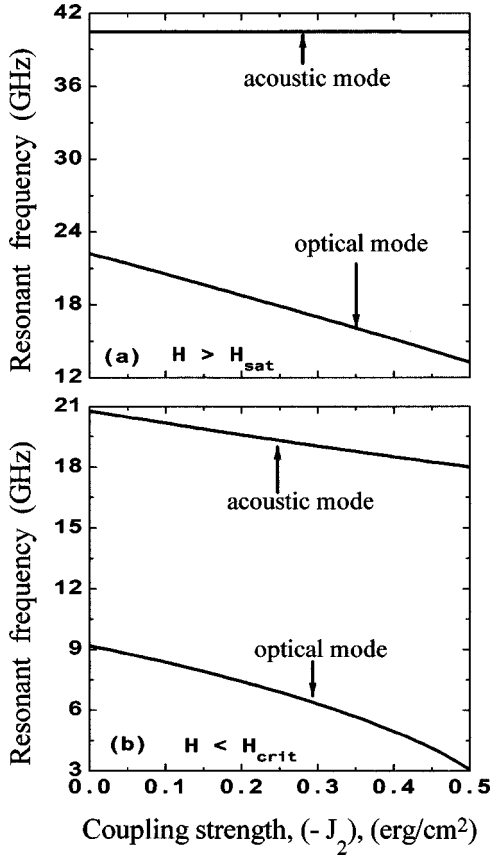


FIG. 5. Resonant frequency vs biquadratic coupling strength $|J_2|$ for antiferromagnetic coupling ($J_1=-2$ erg/cm$^2$). (a) $H=10$ kOe$>H_{\rm sat}$. (b) $H=2$ kOe$<H_{\rm crit}$. Other parameters as in Fig. 1.

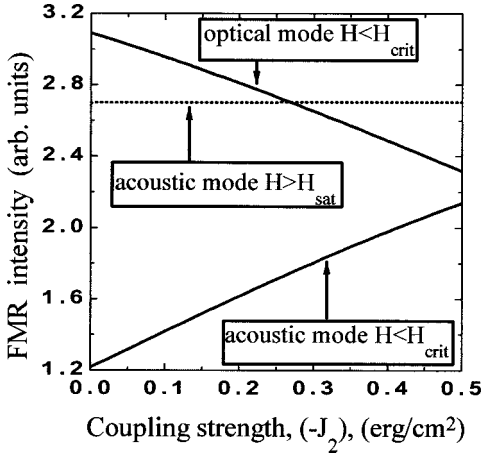


FIG. 6. FMR intensity vs biquadratic coupling strength $|J_2|$ for antiferromagnetic coupling ($J_1=-2$ erg/cm$^2$). Dotted line: $H=10$ kOe$>H_{\rm sat}$. Solid line: $H=2$ kOe$<H_{\rm crit}$. Other parameters as in Fig. 1.

which is the opposite of the ferromagnetic coupling case described above (and also opposite to the resonant field analysis[22]). Two situations can arise. When the applied field $H$ is greater than $H_{\rm sat}$, the magnetizations are parallel; this case is displayed in Figs. 5(a) (resonant frequency) and 6 (dotted line for the mode intensity). One can see that Eq. (4) predicts two modes. The position of the high-frequency (the acoustic) mode does not vary with increasing $|J2|$ [see Fig. 5(a)], while that of the low-frequency (the optical) one decreases almost linearly. However, the latter mode has a zero intensity and the acoustic mode has a constant intensity (see Fig. 6, dotted line). Thus, in practice, only one peak will appear in the FMR spectrum, and, since its position and intensity are constant with $J_2$, it is hard to detect the biquadratic coupling in this case. On the other hand, and for the same parameters, when the magnetizations are antiparallel, the mode behavior is different. In Figs. 5(b) and 6 (solid lines), the applied field, $H=2$ kOe, is less than the critical field $H_{\rm crit}$ (see Sec. III), the magnetizations will align antiferromagnetically under the strong bilinear $J_1$ coupling (assuming $t_AM_A>t_BM_B$, one will have $\phi_A=0°$ and $\phi_B=180°$). Two modes are expected. The mode positions are shown in Fig. 5(b). The resonant frequencies of the lower mode (the optical mode) and the upper (acoustic) mode decrease as $|J_2|$ increases. The corresponding intensities are shown in Fig. 6 (solid lines); note that, contrary to the first case, the intensities of both modes are nonzero and do vary with $J_2$. The intensity of the acoustic (optical) mode will increase (decrease) with $J_2$. Thus, in this case, from the mode position and intensity, one can detect and measure the biquadratic coupling strength.

## VI. CONCLUSION

In summary, the ferromagnetic resonance (FMR) modes are investigated for a trilayer system consisting of two ferromagnetic films interacting through a nonmagnetic interlayer. Included in the model are bilinear $J_1$ and biquadratic $J_2$ couplings and in-plane uniaxial magnetocrystalline anisotropies with anisotropy axis directions in the two layers making a $\delta$ angle. The saturation ($H_{\rm sat}$) and critical ($H_{\rm crit}$) fields and an analytical formula for the mode intensity have been found in terms of $J_1$, $J_2$, and $\delta$. The resonant frequency and the mode intensity are discussed as a function of $J_1$, $J_2$, and $\delta$. For a given positive $J_1$ (ferromagnetic coupling), an additional $J_2$ ($J_2<0$) will lead to an increase (a decrease) of the optical (acoustic) mode intensity. For fixed $J_1<0$ (antiferromagnetic coupling), and if the magnetizations are parallel ($H>H_{\rm sat}$) only the acoustic mode will appear with constant mode position and intensity for all $J_2$ values, making it difficult to detect any additional biquadratic coupling. On the other hand, and for the same parameters, if the magnetizations are antiparallel ($H<H_{\rm crit}$), then two modes are predicted; as $|J_2|$ increases the intensity of the acoustic (optical) mode will increase (decrease) while the resonant frequency of both modes will decrease.

[1] P. Grünberg, Acta Mater. **48**, 239 (2000).
[2] B. Heinrich, Can. J. Phys. **78**, 161 (2000).
[3] J. C. Slonczewski, Phys. Rev. Lett. **67**, 3172 (1991).
[4] U. Rüker, S. Demokritov, B. Tsymbal, P. Grünberg, and W. Zinn, J. Appl. Phys. **78**, 387 (1995).
[5] J. C. Slonczewski, J. Magn. Magn. Mater. **150**, 13 (1995).
[6] M. E. Filipkowski, C. J. Gutierrez, J. J. Krebs, and G. A. Prinz, J. Appl. Phys. **73**, 5963 (1993).
[7] M. Rührig, R. Schäfer, A. Hubert, R. Mosler, J. A. Wolf, S. Demokritov, and P. Grünberg, Phys. Status Solidi A **125**, 635 (1991).
[8] H. J. Elmers, G. Liu, H. Fritzshe, and U. Gradmann, Phys. Rev. B **52**, R696 (1995).
[9] M. D. Stiles, J. Magn. Magn. Mater. **200**, 322 (1999).
[10] B. Heinrich, J. F. Cochran, T. Monchesky, and R. Urban, Phys. Rev. B **59**, 14 520 (1999).
[11] B. Heinrich, M. Kowalewski, and J. F. Cochran, Can. J. Chem. **76**, 1595 (1998).
[12] M. Kowalewski, B. Heinrich, J. F. Cochran, and P. Schurer, J. Appl. Phys. **81**, 3904 (1997).
[13] M. E. Filipkowski, C. J. Gutierrez, J. J. Krebs, and G. A. Prinz, in *Proceedings of the Sixth Joint Magnetism and Magnetic Materials, Intermag Conference, Albuquerque, NM, 20–23 June 1994* [J. Appl. Phys. **76**, 7090 (1995)].
[14] T. L. Monchesky, B. Heinrich, R. Urban, K. Myrtle, M. Klaua, and J. Kirchner, Phys. Rev. B **60**, 10 242 (1999).
[15] A. Layadi, Phys. Rev. B **63**, 174410 (2001).
[16] B. Heinrich, J. F. Cochran, M. Kowelewski, J. Kirschner, Z. Celinski, A. S. Arrot, and K. Myrtle, Phys. Rev. B **44**, 9348 (1991).
[17] Z. Zhang, L. Zhou, P. E. Wigen, and K. Ounadjela, Phys. Rev. B **50**, 6094 (1994).
[18] A. Layadi and J. O. Artman, J. Magn. Magn. Mater. **92**, 143 (1990).
[19] A. Layadi and J. O. Artman, J. Magn. Magn. Mater. **176**, 175 (1997).
[20] Q. Y. Jin, H. R. Zhai, Y. B. Xu, Y. Zhai, M. Lu, S. M. Zhou, J. S. Payson, G. L. Dunifer, R. Naik and G. W. Auner, J. Appl. Phys. **77**, 3971 (1995).
[21] B. Heinrich and J. F. Cochran, Adv. Phys. **42**, 523 (1993).
[22] B. Heinrich, in *Ultrathin Magnetic Structures II*, edited by B. Heinrich and J. A. C. Bland (Springer-Verlag, Berlin, 1994).
[23] B. Heinrich, S. T. Purcell, J. R. Dutcher, K. B. Urquhart, J. F. Cochran, and A. S. Arrot, Phys. Rev. B **38**, 12 879 (1988).
[24] A. Layadi, J. Appl. Phys. **83**, 3738 (1998).
[25] Hideki Watanabe, Eiichi Hirota, Iwao Ishida, Kouichi Hamada, Akira Okada, Hirochi Sakakima, and Mitsuo Satomi, J. Phys. Soc. Jpn. **65**, 3680 (1996).
[26] A. Layadi, J. Magn. Magn. Mater. **192**, 353 (1999).
[27] Z. Celinski, K. B. Urquhart, and B. Heinrich, J. Magn. Magn. Mater. **166**, 6 (1997).
[28] B. Heinrich, K. B. Urquhart, A. S. Arrot, J. F. Cochran, K. Myrtle, and S. T. Purcell, Phys. Rev. Lett. **59**, 1756 (1987).
[29] A. Layadi, J. Appl. Phys. **87**, 1429 (2000).
[30] A. Layadi, J. Appl. Phys. **86**, 1625 (1999).
[31] J. Smit and H. G. Beljers, Philips Res. Rep. **10**, 113 (1955).